Electronic Supplementary Information

Experimental Section

Materials: NH_4F and urea were purchased from Beijing Chemical Works. $Ni(NO_3)_2 \cdot 6H_2O$ was purchased from Aladdin Ltd. (Shanghai, China). $K_2B_4O_7 \cdot 4H_2O$ was provided by Chengdu Kelong Chemical Reagent Factory. Pt/C (10 wt% Pt) was purchased from Alfa Aesar (China) Chemicals Co. Ltd. Nafion (5 wt%) were purchased from Sigma-Aldrich Chemical Reagent Co., Ltd. All reagents were used as received without further purification. Ti mesh was purchased from Phychemsi Hong Kong Company Limited and was cleaned by sonication sequentially in acetone, water and ethanol several times to remove the surface impurities. Ultrapure water was utilized to prepare all solutions.

Preparation of $Ni(OH)_2$ NS/Ti and Ni_3N NS/Ti: $Ni(OH)_2$ NS/Ti was prepared by a simple hydrothermal method. In brief, 2.5 mmol $Ni(NO_3)_2 \cdot 6H_2O$ 10 mmol urea, and 4 mmol NH_4F were dissolved in 40 mL ultrapure water. Then the mixture solution and a piece of cleaned Ti mesh (2 cm × 3 cm) were transferred to a 40 mL Teflon-lined stainless-steel autoclave and maintained at 120 °C for 6 h. After the autoclave cooled down naturally, the resulting $Ni(OH)_2$ NS/Ti was taken out and washed with ultrapure water and dried at 60 °C. To make Ni_3N NS/Ti, $Ni(OH)_2$ NS/Ti was placed in the furnace and heated to 380 °C with a heating speed of 5 °C min^{-1} under a flowing NH_3 atmosphere. After reacting 3 h at 380 °C, the system was allowed to cool down to room temperature naturally still under a flowing NH_3 atmosphere. Finally, the black Ni_3N NS/Ti was collected for further characterization.

Preparation of Ni_3N@Ni-Bi NS/Ti: To obtain Ni_3N@Ni-Bi NS/Ti, the Ni_3N NS/Ti electrode (0.5 × 0.5 cm) was used as the working electrode, Pt wire as the auxiliary electrode and a Ag/AgCl as the reference electrode and polarized at 1.1 V (*vs.* Ag/AgCl) in 0.1 M K-Bi (pH: 9.2) until the current density raises for about 0.5 h until reaching a plateau (Fig. S1).

Characterizations: XRD measurements were performed using a RigakuD/MAX 2550

diffractometer with Cu Kα radiation (λ=1.5418 Å). SEM measurements were carried out on a XL30 ESEM FEG scanning electron microscope at an accelerating voltage of 20 kV. TEM images were collected on a Zeiss Libra 200FE transmission electron microscope operated at 200 kV. XPS measurements were performed using an ESCALABMK II X-ray photoelectron spectrometer with the exciting source of Mg.

Electrochemical measurements: Electrochemical measurements were performed with a CHI 660E electrochemical analyzer (CH Instruments, Inc., Shanghai) in a conventional three electrode system, using Ni_3N@Ni-Bi NS/Ti as working electrode, a platinum wire as counter electrode and saturated calomel electrode as reference electrode. Given that as-measured reaction currents do not directly reflect the intrinsic behavior of catalysts due to the effect of ohmic resistance, an *iR* correction was applied to all LSV curves for further analysis,[1] and all potentials were reported on a reversible hydrogen electrode (RHE) scale unless specifically stated. The potentials were calibrated to RHE, using the following equation: E (RHE) = E (Ag/AgCl) + (0.197 + 0.059 pH) V. Polarization curves were obtained using linear sweep voltammetry with a scan rate of 2 mV s^{-1}.

Computational Methods: All the density-functional theory (DFT) calculations in this study were performed using the Vienna *ab initio* simulation package (VASP).[2-4] We used the PBE functional for the exchange-correlation energy[4] and projector augmented wave (PAW) potentials.[6,7] The kinetic energy cutoff in the calculation was set to 450 eV. The ionic relaxation was performed until the force on each atom is less than 0.03 eV/Å and convergence criteria of total energy were set to 10^{-4} eV. The 3×3×1 k-points meshes were sampled based on the Monkhorst-Pack method.[8] The Hubbard U parameter (GGA + U) with U = 4 eV was used to calculate the electron correlation within the Ni ions. The simulations performed were based on the five-layer thick Ni_3N (110) surface and a periodical Ni-Bi model structure with 24 Ni, 16 boron and 48 oxygen atoms. To minimize the undesired interactions between images, a vacuum of at least 15 Å was considered along the z axis.

Previous studies have shown that the OER activity is strongly correlated with the free energy of O*, OH* and OOH* binding to the electrocatalysts surface. The four

step OER mechanism is proposed as:

$$2H_2O + * \rightarrow OH^* + H_2O + e^- + H^+ \quad (1)$$

$$OH^* + H_2O \rightarrow O^* + H_2O + e^- + H^+ \quad (2)$$

$$O^* + H_2O \rightarrow OOH^* + e^- + H^+ \quad (3)$$

$$OOH^* \rightarrow O_2 + e^- + H^+ \quad (4)$$

The free energy (ΔG_i) for O*, OH* and OOH* adsorption on $Ni_3N$and Ni-Bi surfaces was calculated as follows:

$$\Delta G_i = \Delta E_i + \Delta E_{ZPE} - T\Delta S \quad (5)$$

where ΔE_i is the reaction energy for each elementary step, ΔE_{ZPE} is the zero-point energy change and ΔS is the entropy change. The theoretical overpotential can be defined as:

$$\eta = \max [\Delta G_1, \Delta G_2, \Delta G_3, \Delta G_4]/e - 1.23[V] \quad (6)$$

FE determination: The generated gas was confirmed by gas chromatography (GC) analysis and measured quantitatively using a calibrated pressure sensor to monitor the pressure change in the anode and cathode compartment of a H-type electrolytic cell. The FE was calculated by comparing the amount of measured oxygen/hydrogen generated by potentiostatic anodic/cathode electrolysis with calculated oxygen/hydrogen (assuming 100% FE). GC analysis was carried out on GC-2014C (Shimadzu Co.) with thermal conductivity detector and nitrogen carrier gas. Pressure data during electrolysis were recorded using a CEM DT-8890 Differential Air Pressure Gauge Manometer Data Logger Meter Tester with a sampling interval of 1 point per second.

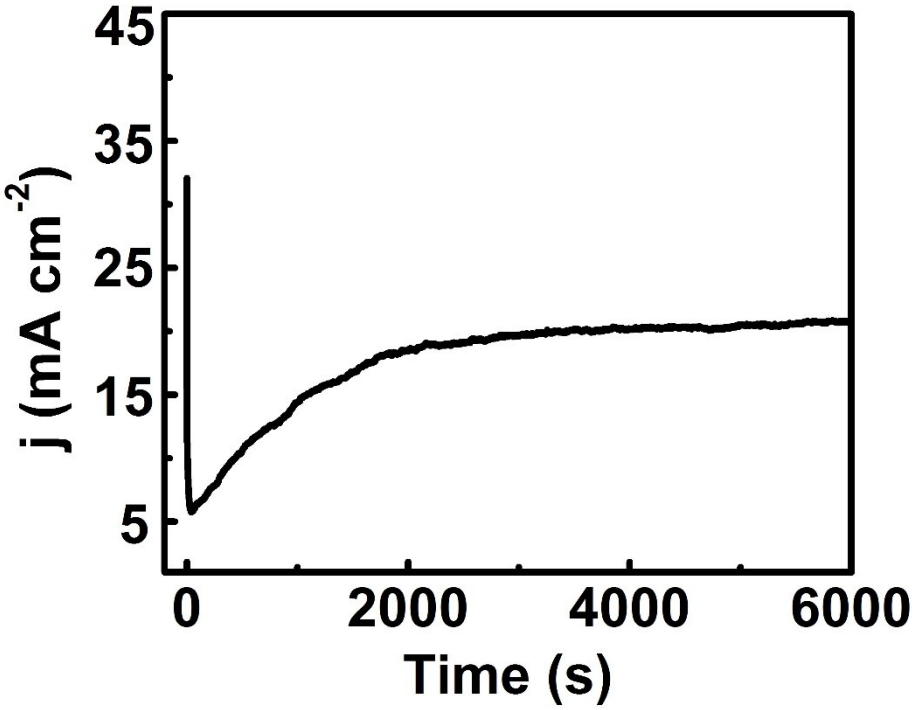

Fig. S1. Time-dependent current density curve for oxidative polarization of Ni_3N@Ni-Bi NS/Ti.

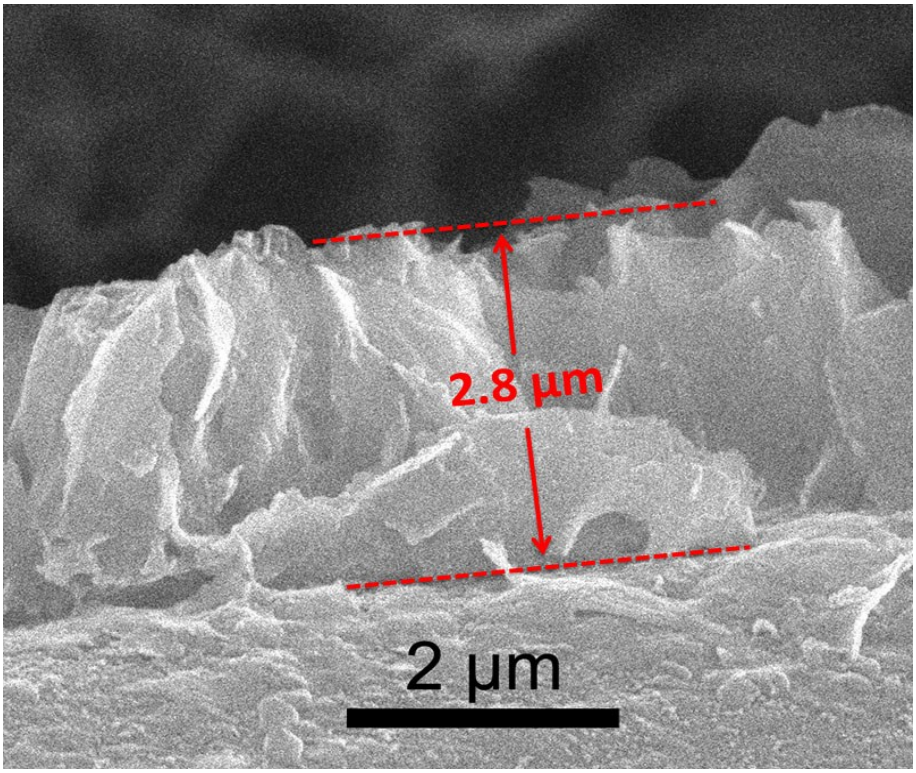

Fig. S2.

Cross-section SEM image of Ni_3N@Ni-Bi NS/Ti.

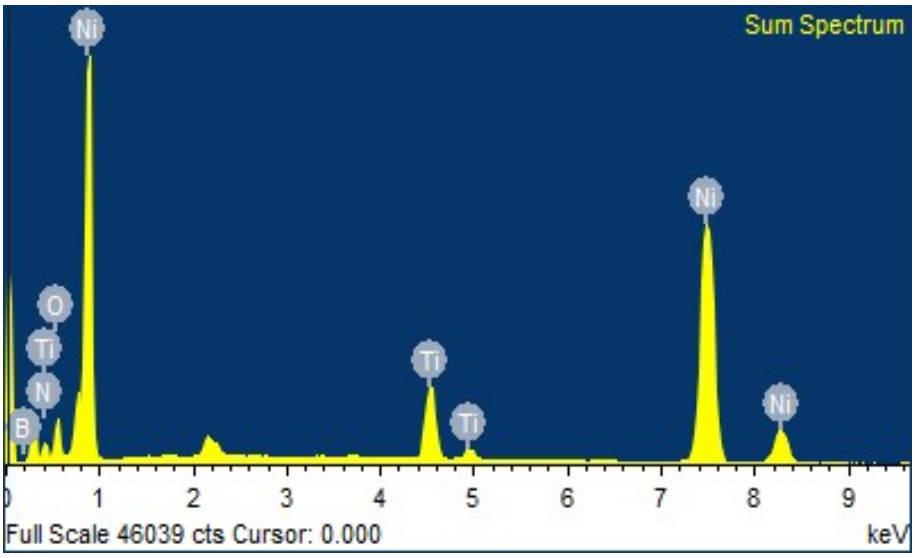

Fig. S3.

EDX spectrum of Ni_3N@Ni-Bi NS/Ti.

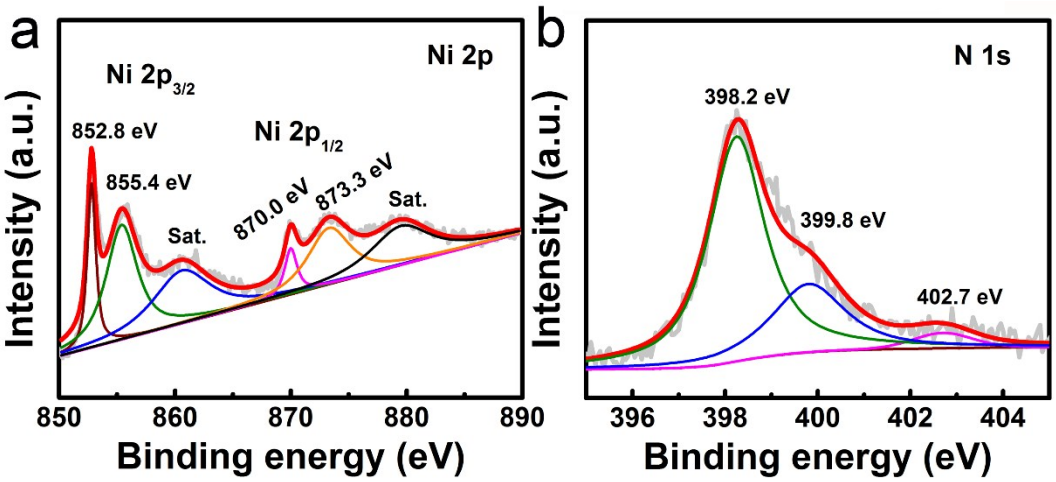

Fig. S4. XPS spectra of Ni_3N in the (a) Ni 2p and (b) N 1s regions.

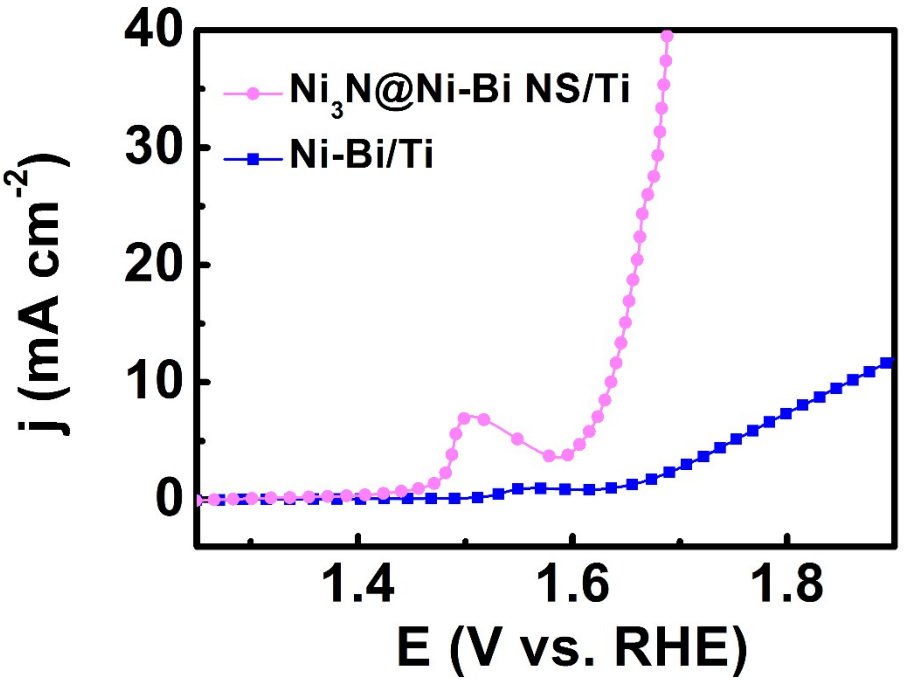

Fig. S5. LSV curves for Ni_3N@Ni-Bi NS/Ti and Ni-Bi/Ti with a scan rate of 2 mV s^{-1} for OER in 0.1 M K-Bi.

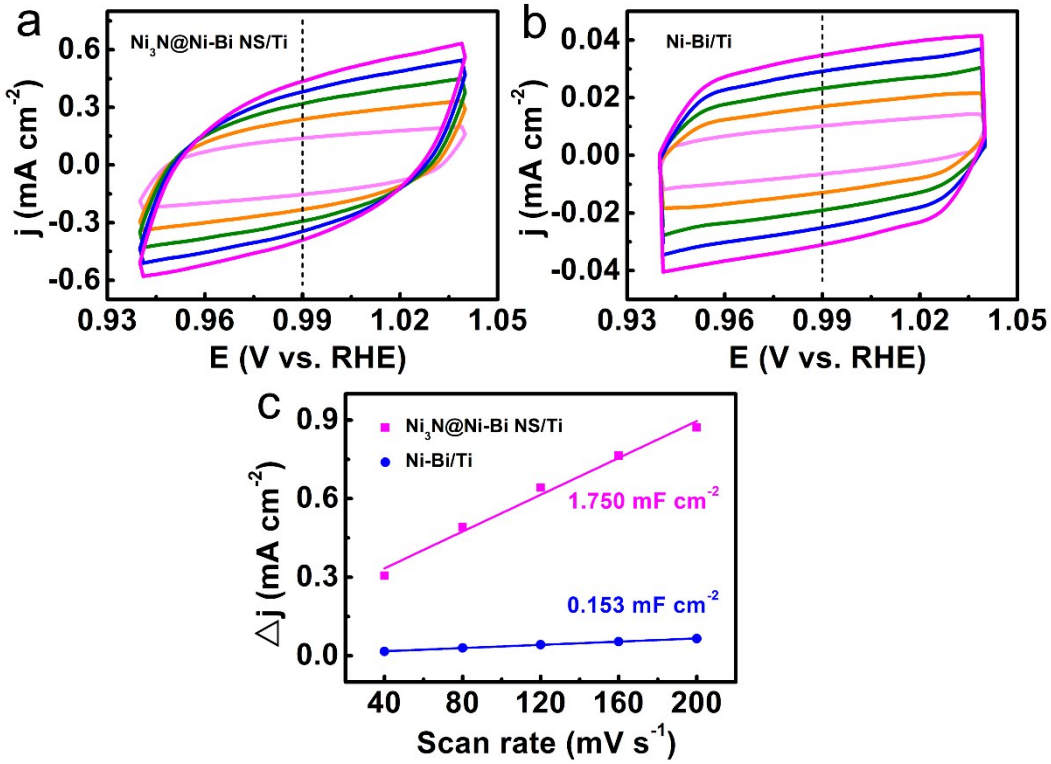

Fig. S6. Cyclic voltammograms for (a) Ni_3N@Ni-Bi NS/Ti and (b) Ni-Bi/Ti in the non-faradaic capacitance current range at scan rates of 40, 80, 120,160, and 200 mV s^{-1}. (c) The capacitive currents at 0.99 V as a function of scan rate for Ni_3N@Ni-Bi NS/Ti and Ni-Bi/Ti.

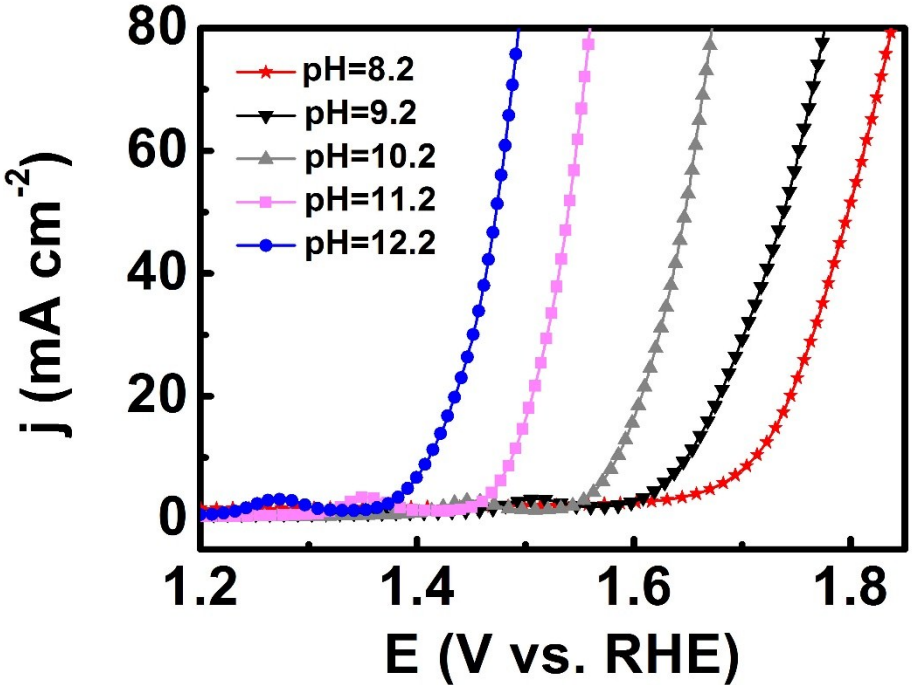

Fig. S7. LSV curves of Ni_3N@Ni-Bi NS/Ti for OER 0.5M K-Bi with different pH.

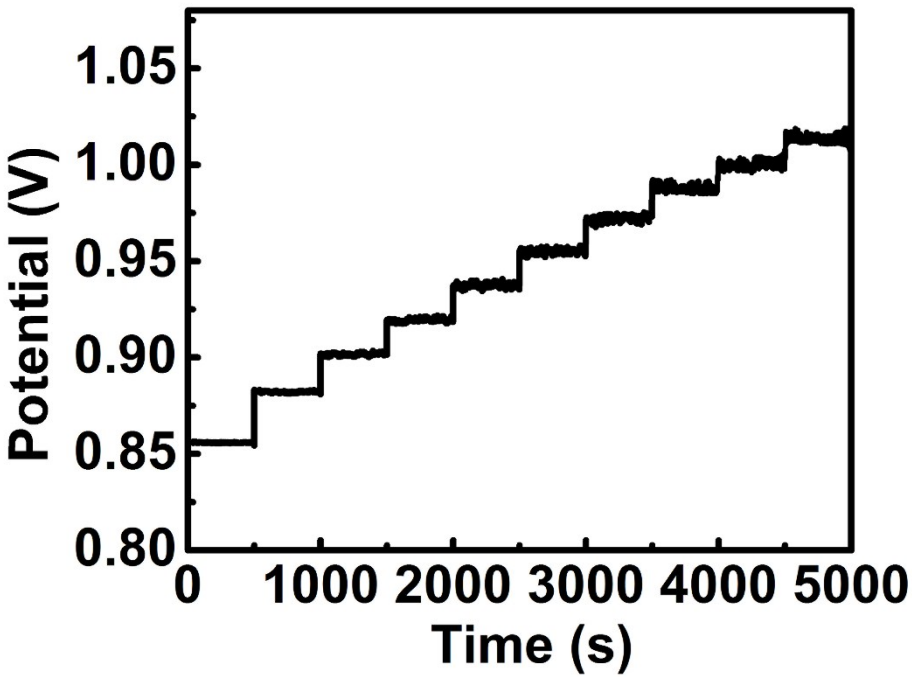

Fig. S8. Multi-current process of Ni_3N@Ni-Bi NS/Ti in 0.5 M K-Bi. The current density started at 4 mA cm^{-2} and ended at 40 mA cm^{-2}, with an increment of 4 mA cm^{-2} per 500 s.

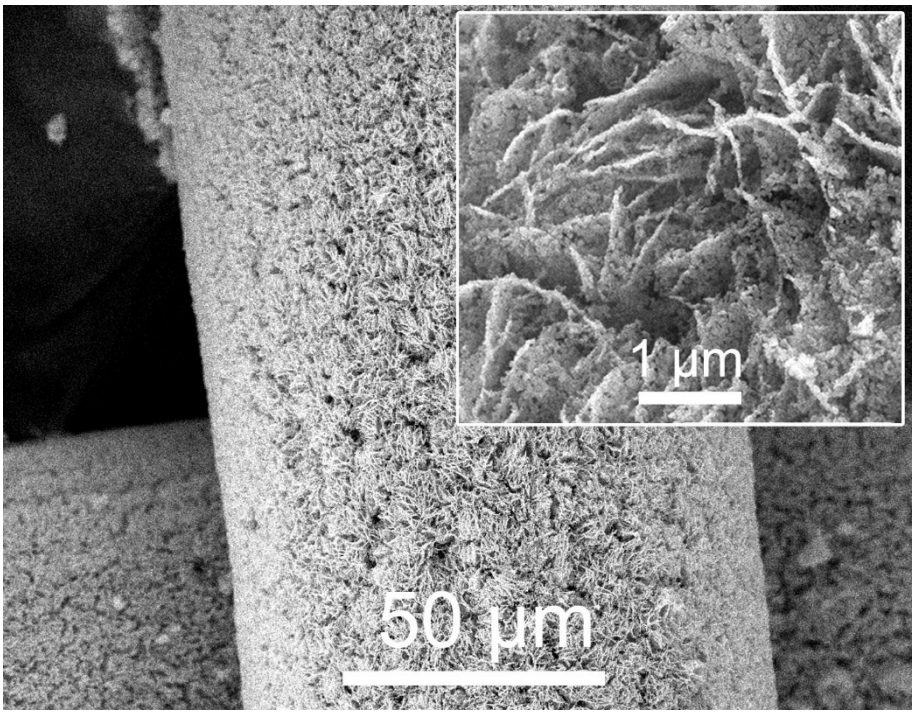

Fig. S9. SEM images for Ni_3N@Ni-Bi NS/Ti after long-term stability test.

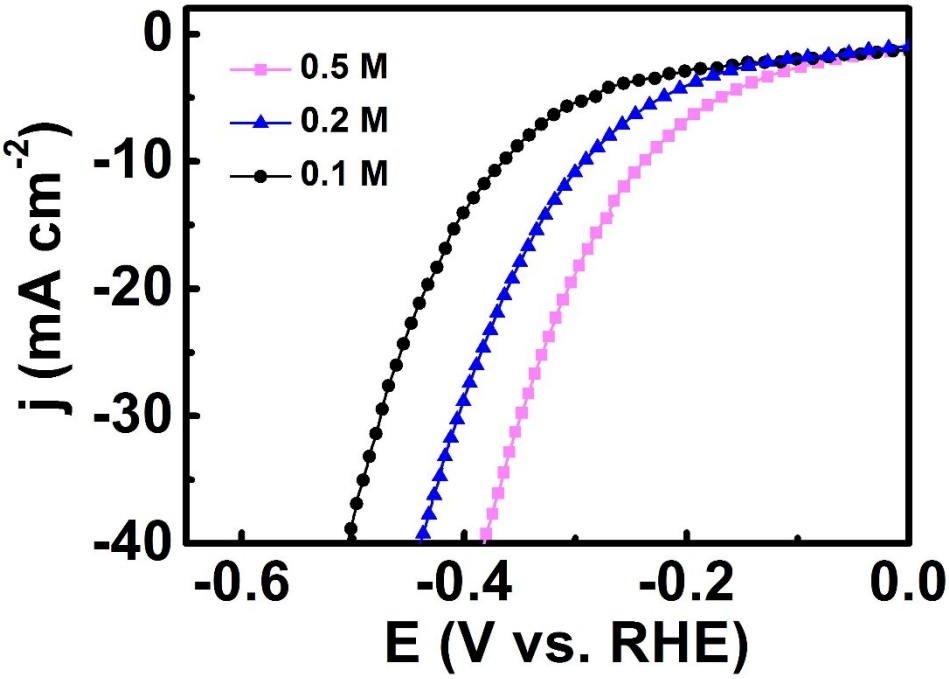

Fig. S10. LSV curves for Ni_3N@Ni-Bi NS/Ti in 0.1, 0.2, and 0.5 M K-Bi with a scan rate of 2 mV s^{-1} for HER.

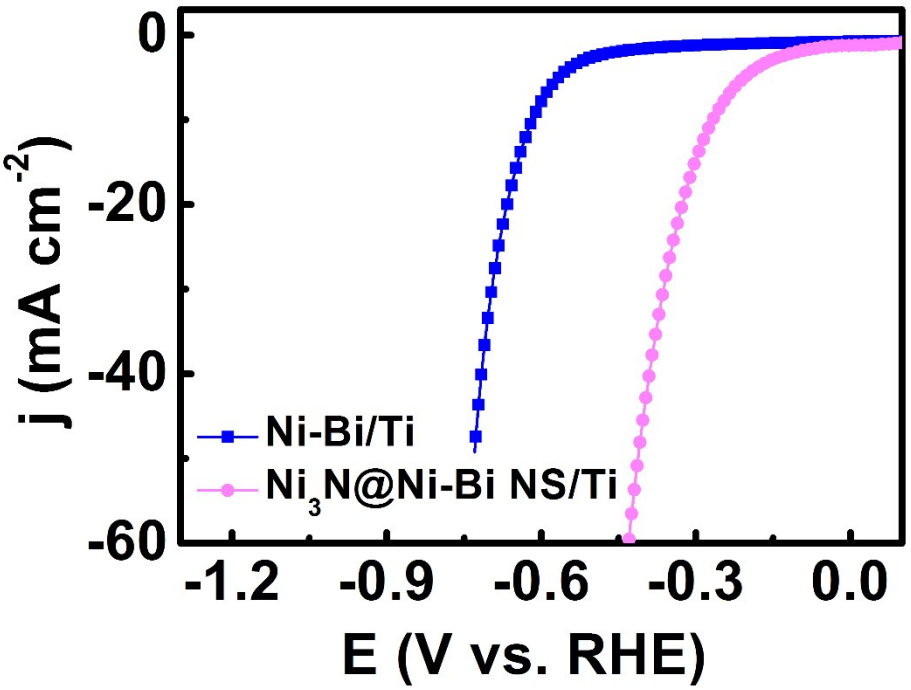

Fig. S11. LSV curves for Ni_3N@Ni-Bi NS/Ti and Ni-Bi/Ti with a scan rate of 2 mV s^{-1} for HER in 0.5 M K-Bi.

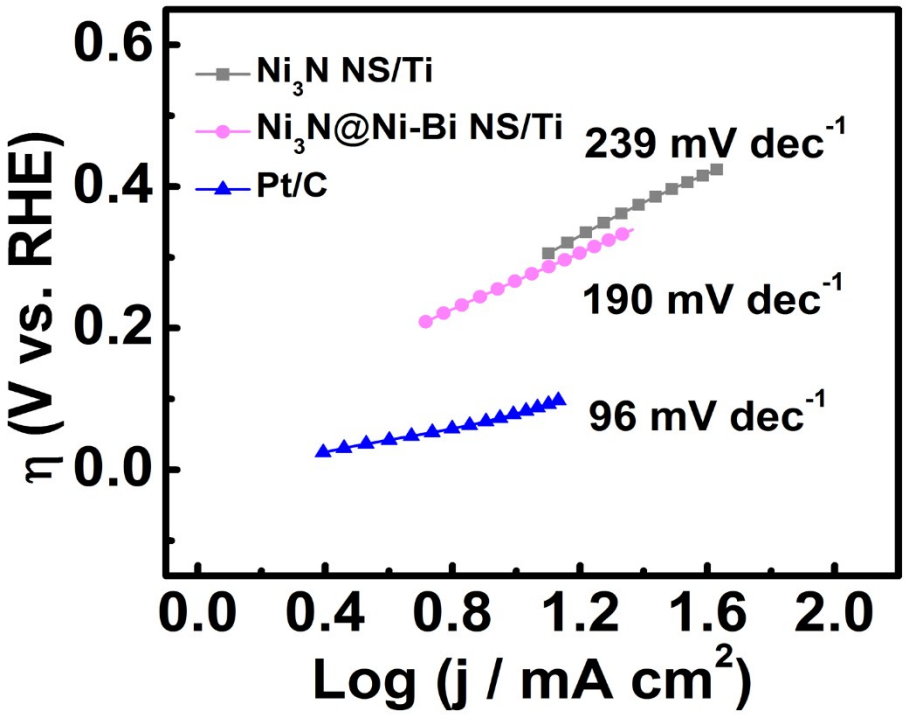

Fig. S12. Tafel plots for Ni_3N@Ni-Bi NS/Ti, Ni_3N NS/Ti, and Pt/C on Ti mesh.

Fig. S13. Water splitting driven by a cell voltage of 1.95 V in 0.5 M K-Bi.

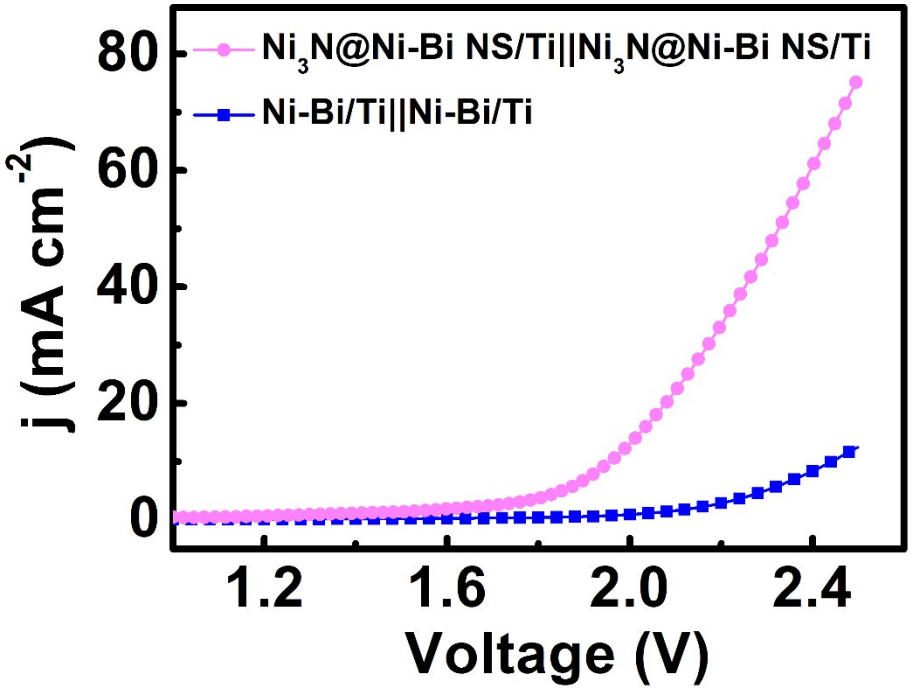

Fig. S14. Polarization curves of Ni_3N@Ni-Bi NS/Ti||Ni_3N@Ni-Bi NS/Ti and Ni-Bi/Ti||Ni-Bi/Ti for overall water splitting with a scan rate of 2 mV s^{-1}.

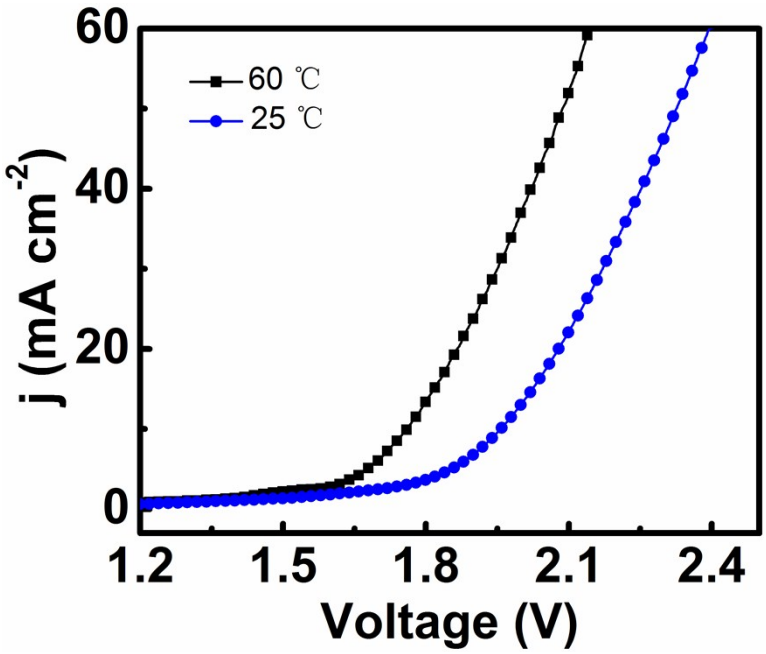

Fig. S15. LSV curves of water electrolysis for Ni_3N@Ni-Bi NS/Ti||Ni_3N@Ni-Bi NS/Ti two-electrode system at 25 and 60 °C.

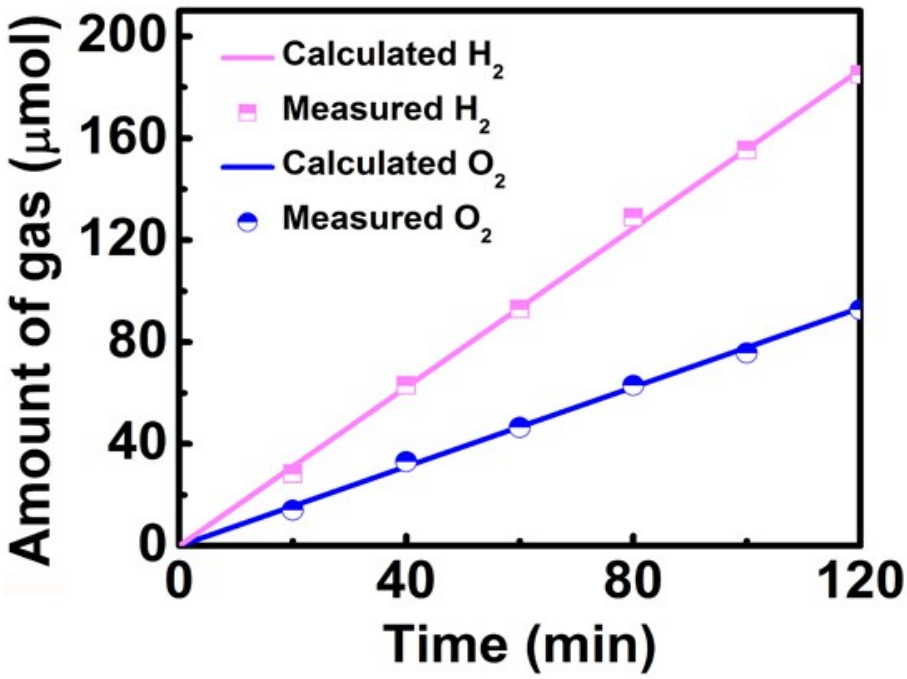

Fig. S16. The amount of gas theoretically calculated and experimentally measured *vs.* time for overall water splitting of Ni_3N@Ni-Bi NS/Ti||Ni_3N@Ni-Bi NS/Ti.

Table S1. Comparison of OER performance in 0.5 M K-Bi for Ni_3N@Ni-Bi NS/Ti with other non-noble-metal electrocatalysts in neutral or near-neutral media.

Catalyst	j (mA cm^{-2})	η (mV)	Electrolyte	Refs.
Ni_3N@Ni-Bi NS/Ti	10	405	0.1 M K-Bi	This work
	10	382	0.5 M K-Bi	
Ni-Bi/Ti	10	630	0.1 M K-Bi	This work
Ni-Bi/FTO	1	384	0.5 M K-Bi	9
Ni-Bi/FTO	1	425	0.1 M BBS	10
Ni-Bi/FTO	1	540	0.5 M K-Bi	11
Ni-Bi film/FTO	1	410	1 M K-Bi	12
Ni-Bi film/FTO	0.6	618	0.1 M Na-Bi	13
NiO_x/MWCNT	0.5	330	0.1 M K-Bi	14
NiO_x-NH_3/FTO	1	560	0.1 M Na-Bi	15
NiO_x-en/FTO	1	510		
NiO_x-Bi	1	650	0.5 M K-Bi	16
NiO_x-Fe-Bi	5	552		
Co-Bi/FTO	1	390	1 M K-Bi	17
Co-W/FTO	1	420	0.05 M K-Bi	18
Fe-Bi/FTO	1	490	0.5 M BBS	19
Fe-Ci/FTO	10	560	0.2 M CBS	20
Cu-Bi/FTO	10	810	0.2 M BBS	21
CuO/FTO	0.1	430	0.1 M K-Bi	22
Cu-TPA/FTO	0.18	320	0.1 M K-Bi	23
CoO_2/$CoSe_2$-Ti	10	510	1.0 M PBS	24
Co-OEC/NF	100	442	1.0 M PBS	25

Table S2. Comparison of HER performance for Ni_3N@Ni-Bi NS/Ti with other non-noble-metal electrocatalysts in neutral or near-neutral media.

Catalyst	j (mA cm^{-2})	η (mV)	Electrolyte	Refs.
Ni_3N@Ni-Bi NS/Ti	10	265	0.5 M K-Bi	This work
	20	340		
Ni-Bi/Ti	10	617	0.5 M K-Bi	This work
Ni-Bi film/FTO	1.5	425	0.1 M Na-Bi	13
Cu-TPA/FTO	1	440	0.1 M K-Bi	23
$CoO_2/CoSe_2$-Ti	10	337	1.0 M PBS	24
Cu-EA/FTO	2	270	0.1 M K-Pi	26
Co-NRCNTs	10	540	0.1 PBS	27
H_2-CoCat/FTO	2	385	0.5 M K-Pi	28
Cu(0) based film	10	333	0.5 M PBS	29
Carbon-armored Co_9S_8 nanoparticle	10	280	1.0 M PBS	30
MoP/CF	1	300	1.0 M PBS	31
FeS	0.7	450	0.1 M PBS	32
CoP/CC	2	65	1.0 M PBS	33

References

1 Z. Xing, Q. Liu, A. M. Asiri and X. Sun, *Adv. Mater.,* 2014, **26**, 5702-5707.

2 G. Kresse and J. Furthmuller, *Comp. Mater. Sci.,* 1996, **6**, 15-50.

3 G. Kresse and J. Furthmuller, *Phys. Rev. B,* 1996, **54**, 11169-11186.

4 G. Kresse and J. Hafner, *Phys. Rev. B,* 1994, **49**, 14251-14269.

5 J. P. Perdew, K. Burke and M. Ernzerhof, *Phys. Rev. Lett.,* 1997, **78**, 1396-1396.

6 G. Kresse and D. Joubert, *Phys. Rev. B,* 1999, **59**, 1758-1775.

7 P. E. Blochl, *Phys. Rev. B,* 1994, **50**, 17953-17979.

8 H. J. Monkhorst and J. D. Pack, *Phys. Rev. B,* 1976, **13**, 5188-5192.

9 D. K. Bediako, Y. Surendranath and D. G. Nocera, *J. Am. Chem. Soc.,* 2013, **135**, 3662-3674.

10 M. Dinca, Y. Surendranath and D. G. Nocera, *Proc. Natl. Acad. Sci. U.S.A.,* 2010, **107**, 10337–10341.

11 I. M. Roger and D. Symes, *J. Am. Chem. Soc.,* 2015, **137**, 13980-13988.

12 D. K. Bediako, B. Lassallekaiser, Y. Surendranath, J. Yano, V. K. Yachandra and D. G. Nocera, *J. Am. Chem. Soc.,* 2012, **134**, 6801-6809.

13 C. He, X. Wu and Z. He, *J. Phys. Chem. C,* 2014, **118**, 4578-4584.

14 X. Yu, T. Hua, X. Liu, Z. Yan, P. Xu and P. Du, *ACS Appl. Mater. Interfaces,* 2014, **6**, 15395-15402.

15 A. Singh, S. L. Y. Chang, R. K. Hocking, U. Bach and L. Spiccia, *Energy Environ. Sci.,* 2013, **6**, 579-586.

16 A. M. Smith, L. Trotochaud, M. S. Burke and S. W. Boettcher, *Chem. Commun.,* 2015, **51**, 5261-5263.

17 A. J. Esswein, Y. Surendranath, S. Y. Reece and D. G. Nocera, *Energy Environ. Sci.,* 2011, **4**, 499-504.

18 B. Zhang, X. Wu, F. Li, F. Yu, Y. Wang and L. Sun, *Chem. Asian J.,* 2015, **10**, 2228-2233.

19 D. R. Chowdhury, L. Spiccia, S. S. Amritphale, A. Paul and A. Singh, *J. Mater. Chem. A,* 2016, **4**, 3655-3660.

20 F. Li, L. Bai, H. Li, Y. Wang, F. Yu and L. Sun, *Chem. Commun.,* 2016, **52**, 5753-5756.

21 F. Yu, F. Li, B. Zhang, H. Li and L. Sun, *ACS Catal.,* 2015, **5**, 627-630.

22 X. Liu, S. Cui, Z. Sun and P. Du, *Electrochim. Acta,* 2015, **160**, 202-208.

23 X. Liu, H. Zheng, Z. Sun, A. Han and P. Du, *ACS Catal.,* 2015, **5**, 1530-1538.

24 K. Li, J. Zhang, R. Wu, Y. Yu and B. Zhang, *Adv. Sci.,* 2016, **3**, 1500426.

25 A. J. Esswein. Y. Surendranath, S. Y. Reece and D. G. Nocera, *Energy Environ. Sci.,* 2011, **4**, 499-504.

26 X. Liu, S. Cui, Z. Sun and P. Du, *Chem. Commun.,* 2015, **51**, 12954-12957.

27 X. Zou, X. Huang, A. Goswami, R. Silva, B. R. Sathe, E. Mikmeková and T. Asefa, *Angew. Chem., Int. Ed.,* 2014, **53**, 4372-4376.

28 S. Cobo, J. Heidkamp, P. Jacques, J. Fize, V. Fourmond, L. Guetaz, B. Jousselme, V. Ivanova, H. Dau, S. Palacin, M. Fontecave and V. Artero, *Nat. Mater.,* 2012, **11**, 802-807.

29 J. Du, J. Wang, L. Ji, X. Xu and Z. Chen, *ACS Appl. Mater. Interfaces,* 2016, **8**, 30205-30211.

30 L. Feng, G. Li, Y. Liu, Y. Wu, H. Chen, Y. Wang, Y. Zou, D. Wang and X. Zou, *ACS Appl. Mater. Interfaces,* 2015, **7**, 980-988.

31 W. Cui, Q. Liu, Z. Xing, A. M. Asiri, K. A. Alamry and X. Sun, *Appl. Catal. B-Environ.,* 2015, **164**,144-150.

32 C. D. Giovanni, W.-A. Wang, S. Nowak, J.-M. Greneche, H. Lecoq, L. Mouton, M. Giraud and C. Tard, *ACS Catal.,* 2014, **4**, 681-687.

33 J. Tian, Q. Liu, A. M. Asiri and X. Sun, *J. Am. Chem. Soc.,* 2014, **136**, 7587-7590.